Chapter 6

Optimal Designing Grid-Connected PV Systems

Ali Reaz Reisi and Ashkan Alidousti

Additional information is available at the end of the chapter

http://dx.doi.org/10.5772/intechopen.79685

Abstract

Photovoltaic systems, direct conversion of solar energy to electrical energy, are produced in the form of DC power by photovoltaic arrays bathed in sunlight and converted into AC power through an inverter system, which is more convenient to use. There are two main paradigms for optimal designing of photovoltaic systems. First, the system can be designed such that the generated power and the loads, that is, the consumed power, match. A second way to design a photovoltaic system is to base the design on economics, as pinpointed in the following. Photovoltaic grid connected through shunt active filter by considering maximum power point tracking for these systems is known as the optimal design. This chapter is organized as follows: First, we discuss an overview of grid-connected photovoltaic systems. After that, we take a more detailed look on grid-connected photovoltaic system via active filter; in this section, we explain the modeling of photovoltaic panel and shunt active filter. In the next section, we learn different maximum power point tracking methods and also learn how to design DC link as a common bus of shunt active filter and photovoltaic system. Finally, MATLAB/Simulink simulations verify the performance of the proposed model performance.

Keywords: optimal designing, grid-connected, photovoltaic systems, shunt active filter, maximum power point tracking

1. Introduction

Global warming, environmental pollution, and possible scarcity of fossil fuel reserves are some of the main driving forces behind the urge for installing grid-connected photovoltaic (PV) systems. Moreover, utilities and customers can benefit from installing these systems. The main gain for customers is to take advantage of the incentives provided by the governments upon

installing PV systems. For utilities, the gains of installing PV systems are mainly operational benefits, especially if the PV system is installed at the customer side on rural feeders. For example, PV systems can be used to decrease the feeder losses, improve the voltage profile of the feeder, and reduce the lifetime operation and maintenance costs of transformer load tap changers. Moreover, if the peak output of the PV system matches the peak loading of the feeder, then the loading of some transformers present in the network can be reduced during peak load periods. The power-quality index of the grid could be improved if PV system was connected to grid via active filters; they are energy conditioners, which include DC/AC-controllable converters. These filters, based on their control schemes, can compensate both source voltage deficiencies and undesirable load-terminal current, which leads to have a source end purely sinusoidal current.

Current harmonic drawn by direct PV grid connected via DC/AV inverters and also nonlinear loads disturb the waveform of the voltage at the point of a common coupling (PCC) and lead to voltage harmonics. Therefore, it is necessary to develop techniques to reduce all the harmonics as it is recommended in the IEEE 519–1992 standard [1]. The first approach consists of the design of LC filters. However, passive filters are not well adapted as they do not take into account the time variation of the loads and the network. They can also lead to resonance phenomena. So, since several years, a more interesting technique is studied: the active filter based either on voltage source or on current source inverters, yielding the harmonic currents required by the load.

Recently, efforts [1, 2] have been made to combine the active filters with renewable energy production systems to benefit from advantages of both a renewable source of energy and a power conditioner to provide pollution-free and high-quality power to the consumers. It seems that it is necessary to use power conditioners, for example, active filters, to compensate the power-quality problems caused by renewable sources of energy in some cases. Since passive filter like LC filters lack the capability to fully compensate these problems in the presence of nonlinear loads, they are not preferred rather than active filters. This type of modular and renewable technology has many advantages like the capability to be expanded and being practically applied in almost everywhere. Furthermore, since one less converter is used in this scheme, there will be capital investment saving in comparison with a separated shunt active filter (SAF) and a PV system; since here by a common DC bus for both SAF and PV systems is used, the cost of the produced power will be reduced.

2. Models of PV and SAF

2.1. PV model

The equivalent circuit of a PV cell is presented in **Figure 1**. Photovoltaic cells of a solar panel have three kinds of external connections, namely series, parallel, and series-parallel. Eq. (1) presents voltage-current characteristic of a solar panel [1], and I_{pv} and I_o are calculated based on the following:

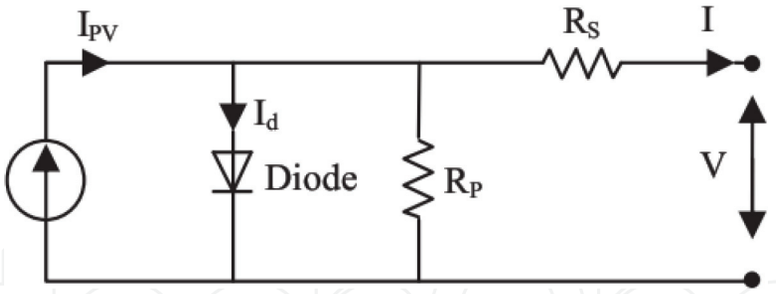

Figure 1. Equivalent circuit of a PV cell.

$$I = I_{PV} - I_O\left[\exp\left(\frac{V + R_S I}{aV_t}\right) - 1\right] - \frac{V + R_S I}{R_p} \tag{1}$$

$$I_{PV} = (I_{PV,n} + K_I \Delta T)\frac{G}{G_n} \tag{2}$$

$$I_O = \frac{I_{SC,n} + K_I \Delta T}{\exp(V_{OC,n} + K_V \Delta T)/aV_t - 1} \tag{3}$$

where I_{PV} and I_o are the photovoltaic current and saturated reverse current, respectively, while "a" and "K" are the ideal diode constant and Boltzmann constant, respectively. Also, we have $V_t = N_S KTq^{-1}$ which is the thermal voltage, N_S is the number of series cells, q is the electron charge, and T is the temperature of p-n junction. R_S and R_P are series and parallel equivalent resistance of the solar panels, respectively. I_{PV} is varied with light intensity in a linear relation and also varies with temperature variations. I_O is dependent on temperature variations.

We have $I_{PV,n}$, $I_{SC,n}$, and $V_{OC,n}$ which are photovoltaic current, short-circuit current (SCC), and open-circuit voltage (OCV) in standard conditions (T_n = 25°C and G_n = 1000 Wm^{-2}), respectively. K_I stands for the coefficient of short-circuit current to temperature, $\Delta T = T - T_n$presents the temperature deviation from standard temperature, G is the light intensity, and K_V shows the ratio coefficient of open-circuit voltage to temperature.

Three important points of I-V characteristic of solar panels are open-circuit voltage, short-circuit current, and voltage-current corresponding to the maximum power. The mentioned points are varied by changes in atmospheric conditions. Short-circuit current and open-circuit voltage can be calculated in different atmospheric conditions by using Eqs. (4) and (5) which are derived from PV model equations, as follows:

$$I_{SC} = (I_{SC,n} + K_I \Delta T)\frac{G}{G_n} \tag{4}$$

$$V_{OC} = V_{OC,n} + K_V \Delta T \tag{5}$$

2.2. SAF

SAF is used to eliminate load-terminal current harmonics and consequently having a pure sinusoidal source-end current. The Generalized Theory of Instantaneous Power (GTIP) theory,

as control algorithm, is used for generating reference signal in the activating algorithm of the shunt active filter [3].

U(t) is assumed as the load voltage which consists of all voltage sequences ($U(t) = U^{+}(t) + U^{-}(t) + U^{0}(t)$, in which $U^{+}(t)$, $U^{-}(t)$, and $U^{0}(t)$ are positive, negative, and zero sequences of $U(t)$), respectively. As a result, using the Optimal Solution theory (OS theory), the source-end current can be rewritten as

$$\begin{cases} \begin{cases} i_g(t) = i_g^{+}(t) + i_g^{-}(t) + i_g^{0}(t) \\ i_g^{+}(t) = \lambda \cdot U^{+}(t) \\ i_g^{-}(t) = \lambda \cdot U^{-}(t) \\ i_g^{0}(t) = \lambda \cdot U^{0}(t) \\ \lambda = \dfrac{\overline{P}(t)}{U(t).U(t)} \end{cases} \\ \begin{cases} i_g(t) = \dfrac{\overline{P}_g(t)}{U(t).U(t)} U(t) \\ i_C(t) = i_{Load}(t) - \dfrac{\overline{P_g}(t)}{U(t).U(t)} U(t) \end{cases} \end{cases} \tag{6}$$

where $i_g(t)$, $i_c(t)$, $i_{Load}(t)$, λ, and $P_g(t)$ are the source current, the compensation current, the current that must be compensated, the instantaneous power factor, and the instantaneous power, in the same order. In Eq. (6), $U(t)$ is the source of distortion due to the fact that it is non-sinusoidal.

Distorted current will be injected by the SAF compensation algorithm. For this reason, the compensation algorithm derived from the GTIP under the two asymmetric and distorted three-phase load-terminal voltages supplies unacceptable outcomes. To tackle these problems, a solution is adopted on the basis of A-GTIP theory.

In other words, a non-sinusoidal load current in addition to $i^{+}(t)$ is composed of $i^{-}(t)$ and $i^{0}(t)$. Negative and zero sequences must be supplied with SAF and positive sequence with source ($i_g(t)$). But due to U (t) is non-sinusoidal and consist of positive, negative and zero sequences, based on equation (6), the calculate $i_c(t)$ (SAF injected currents) cannot remove total negative and zero sequences of $i_g(t)$. This means compensation is not optimal.

- One suggestion to overcome voltage asymmetry is to replace U (t) by U^{+} (t) in Eq. (6). Hence, the new source-end currents and the SAF-injected currents are obtained as follows:
- The source-end currents remain purely sinusoidal, while $U^{+}(t)$ does not include any harmonic components. Apart from that, the non-sinusoidal $U^{+}(t)$ in the term U^{+} (t) acts as the source of distortion. Therefore, the SAF compensation algorithm will inject a distorted current. The SAF new-injected current will cause sinusoidal source-end currents in four-wire systems as follows:

$$i_g(t) = \frac{\overline{P_g}(t)}{U_1^+(t).U_1^+(t)} U_1^+(t)$$
$$i_C(t) = i_{Load}(t) - \frac{\overline{P}_g(t)}{U_1^+(t).U_1^+(t)} U_1^+(t) \quad (7)$$

In which $U_1^+(t)$ is the fundamental component of $U^+(t)$. The SAF-controller block diagram is shown in **Figure 2**.

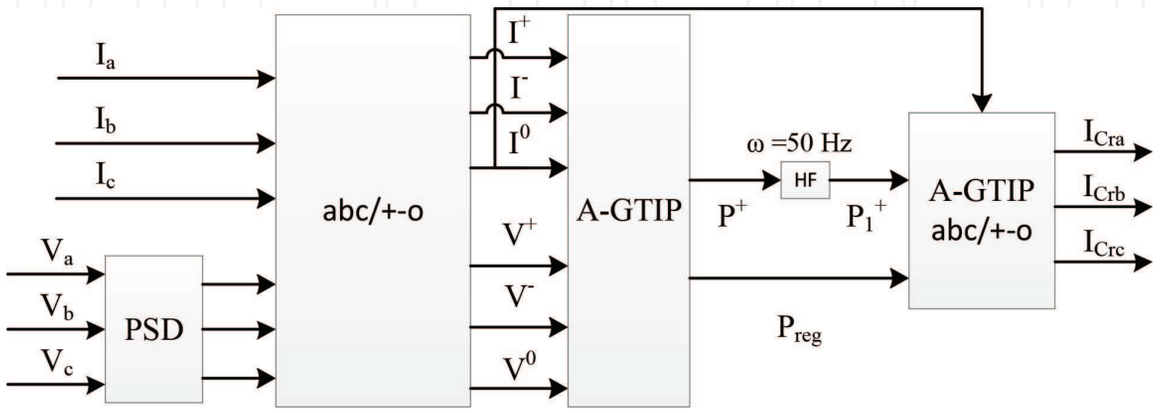

Figure 2. A SAF controller block diagram [1].

In this section, how the PV cells and SAF can be modeled has been explained; in the next section, how the grid-connected PV system and SAF can be related and the proposed block diagram will be presented.

3. SAF-PV system

Figure 3 illustrates the operating principle and current wave form I_{Load} at the load. The PV system is modeled as two parallel current sources. The first one, I_{PV}, is proportional to the

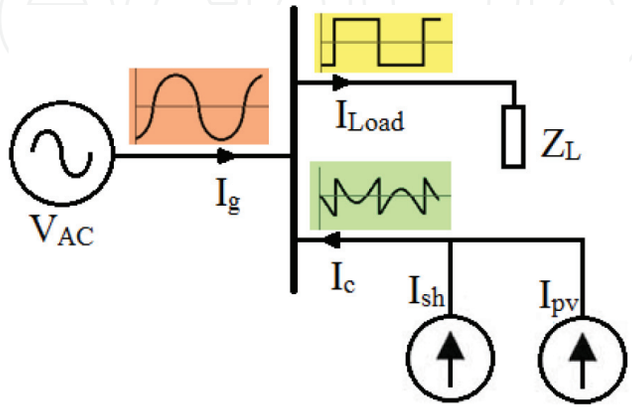

Figure 3. The operating principle of a SAF-PV system.

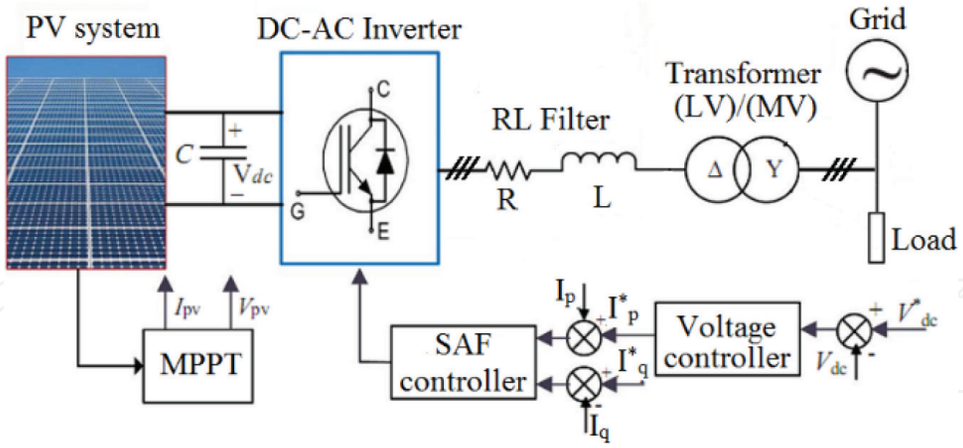

Figure 4. A schematic diagram of the single-stage SAF-PV system.

maximum power available from the PV cells, and its frequency and phase are equal to those of the voltage of the mains. The second current source supplies a wave form, which is equal to the total amount of the harmonics drawn by the load. The current supplied by the mains, I_g, is a purely sinusoidal wave, and the PV system reacts as an active filter to some of the active power and harmonic currents drawn by the load.

The schematic diagram of **Figure 4** shows the power stage of the grid-connected single-stage PV system. It includes the PV array, maximum power point tracking (MPPT) technique, which was used to extract the maximum available power from the PV array, and the DC-link capacitors that connect to the output terminal of the PV array. In addition, a three-phase VSI with its control is based on SAF, RL filter, which is connected to the low voltage AC grid, and a step-up transformer-connected distribution side of the grid.

The design of SAF incorporated with PV system can be decomposed into two issues: (1) maximum power point tracking (MPPT) of the PV system and (2) a control strategy of the voltage of the DC link (V_{DC}) common between SAF and PV systems.

3.1. MPPT

The relatively higher cost required for generating this type of energy in comparison with the energy produced by conventional power generation systems or other renewable sources such as wind power is known as the main disadvantage of the PV systems. Therefore, the optimal operation of the PV systems is critical and achieved by maximizing the efficiency of power delivered to the output by tracking the maximum power point. The PV system is connected to the grid via DC-DC converters. MPPT in PV systems is achieved by applying a control signal to the converters and regulating the PV terminal voltage (or current).

MPPT not only enables an increase in the power delivered from the PV module to the load but also enhances the operating lifetime of the PV system [4]. The solar cell maximum output power at the appropriate operating point and a given cell efficiency depend on the radiation intensity, ambient temperature, and load impedance. It is essential to ensure the efficient operation of the solar cell array that there is a single operating point in which through

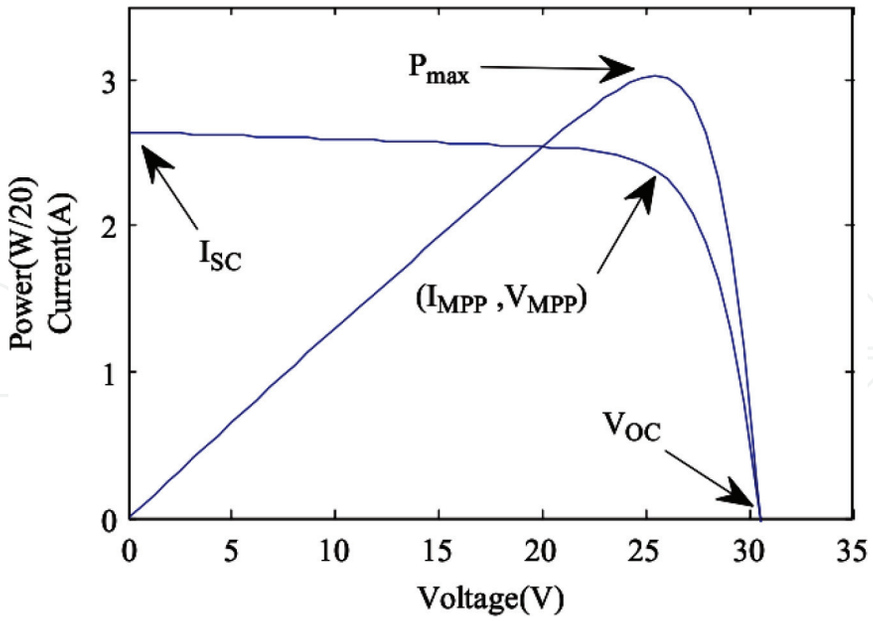

Figure 5. I-V and P-V characteristics of solar cell.

variations in radiation intensity and temperature, the maximum power point tracking is achieved (**Figure 5**). The problematic aspect of MPPT is that PV arrays automatically produce a maximum output power determined by PV output voltage or output current under a given temperature and irradiance. The maximum power attainment involves the adjustment of a load line under variations in temperature and irradiation level.

A wide variety of algorithms and methods have been proposed and implemented to attain MPP tracking [4–6], categorized namely offline methods, online methods, and hybrid methods. Offline methods are dependent on solar cell models, online methods do not specifically rely on the modeling of the solar cell behavior, and hybrid methods are a combination of the two abovementioned methods. On the other hand, the offline and online methods can also be referred to as the model-based and model-free methods, respectively.

3.1.1. Offline methods

In case of offline methods, it is generally required to know one or more of the solar panel values, such as the open-circuit voltage, V_{OC}, short-circuit current, I_{SC}, temperature, and irradiation. Voc and I_{SC} are two values that can be calculated based on measurement of the solar irradiance and temperature or be measured by applying an open circuit or a short circuit to the PV system. While the accuracy of the calculated values is limited by the accuracy of the PV characteristic provided by the manufacturer's specifications, the latter approach does not involve the load interruption necessary for measuring the V_{OC} and I_{SC}. The two values, V_{OC} and I_{SC}, are employed to generate the control signal, which is necessary for driving the solar cell to its maximum power point (MPP). In the course of the tracking of maximum power point operation, the abovementioned control signal remains constant if ambient conditions can be regarded as fixed and there are no attempts to regulate the output power of the PV system.

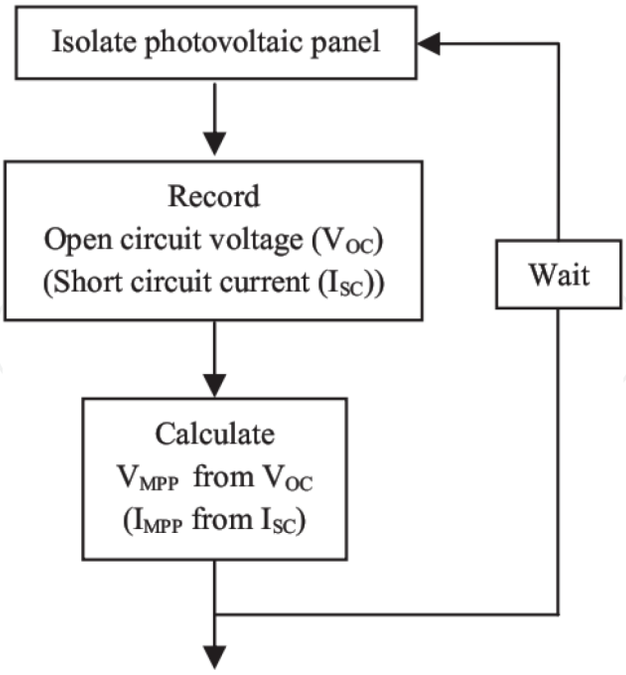

Figure 6. A flowchart of open-circuit voltage (short-current circuit) method [4].

The offline methods known as open-circuit voltage method (OCV), short-circuit current method (SCC), as well as the MPPT method based on artificial intelligence (AI) take variables such as temperature and irradiation as input and calculate the MPP. I_{SC} and V_{OC} can be measured or calculated based on mathematical models provided by the manufacturer or based on experimental data, which reflect the dependence on temperature or irradiance. AI models extract learning-based models using the known relationship between OCV or SCC and temperature and/or irradiance. A flowchart of these methods, which are the simplest offline methods, is depicted in **Figure 6**.

Both of OCV and SCC methods cannot deliver the maximum output power to the load because of two reasons. First, load interruption occurs during the measurement of I_{SC} or V_{OC}, and the second reason is that MPP can never be tracked quite exactly using these methods in the first place as suggested by approximately linear relationship between the open-circuit voltage V_{OC} and V_{MPP} or I_{SC} and I_{MPP}.

These two methods cannot be categorized as "true seeking" MPP methods; however, the simplicity of these algorithms and the ease with which they can be implemented make them suitable for use as part of novel hybrid methods [7, 8].

Artificial intelligence (AI) techniques, as other offline methods, are becoming popular as alternative approaches to conventional techniques or as components of integrated systems. They have been used to solve complicated practical problems in various areas. In [9], only the applications of artificial neural networks (ANNs) and fuzzy logic (FL) are discussed, while AI techniques consist of several disciplines.

The ANN-based method advantage lies with the fact that the trained neural network can provide a sufficiently accurate MPPT without requiring extensive knowledge about the PV

parameters. Most of PV arrays exhibit different output characteristics; however, it must be mentioned that an ANN has to be specifically trained for the PV array with which it will be used. The time-varying characteristics of a PV array imply that the neural network has periodically trained to be guaranteed to track MPP accurately. Implement training periodically needs collecting data, which is a time-consuming process.

Fuzzy logic controllers take full advantages of the following: the ability to work with imprecise inputs, the requirement shortage of an accurate mathematical model, the ability to handle nonlinearity, and fast convergence. However, the approximation of achieving learning ability and accuracy depends on the fuzzy level number and the membership functions form. In most fuzzy systems, there is a connection between membership function, fuzzification and defuzzification, as well as the antecedent and the consequent fuzzy rules that are determined through trial and error, which can take a long time to perform.

3.1.2. Online methods

In case of online methods, the control signals are usually generated by using the instantaneous values of the PV output voltage or current. The control signal is applied to the PV system along with a small methodical and premeditated perturbation in voltage or current or duty cycle (control signal), and the resulting output power is determined. By analyzing perturbation response on the output power of a PV panel, the direction in which the control signal changes (decrease or increase) is determined. Hence, in contrast to the offline methods, the control signal can no longer be regarded as constant when a perturbation is applied. Therefore, the maximum output power tracking involves some oscillations around the optimum value.

In online methods, also known as model-free methods, control signals are usually generated by the instantaneous values of the PV output voltage or current. The more known online methods are Perturbation and Observation method (P&O), Extremum Seeking Control method (ESC), and the Incremental Conductance method (IncCond).

P&O method is considered by a number of researchers due to the fact that it is one of the simplest online methods [10]. P&O can be implemented by applying perturbations to the reference voltage or the reference current signal of the solar panel. **Figure 7** depicts this method's flowchart, which is also known as the "hill climbing method," where "X" is the reference signal. In the algorithm, taking the reference signal, X, as the voltage, (i.e., X = V), the goal will involve pushing the reference voltage signal toward $V_{MPP,}$ thereby causing the instantaneous voltage to track the V_{MPP}. As a consequence, the output power will approach the maximum power point. With this end in view, a small but constant perturbation is applied to the solar panel voltage.

A systematic ECS methodology supported by rigorous theories such as averaging and singular perturbation was recently presented. This real-time optimization methodology involves a nonlinear dynamic system with an adaptive feedback. This ESC method has been successfully applied in PV systems in order to track MPP [11]. With the self-optimizing extremum algorithm as the MPPT controller, the control objective is for the PV system operating point to rapidly trace the MPPs subject to uncertainties and disturbances from the PV panel and the external load.

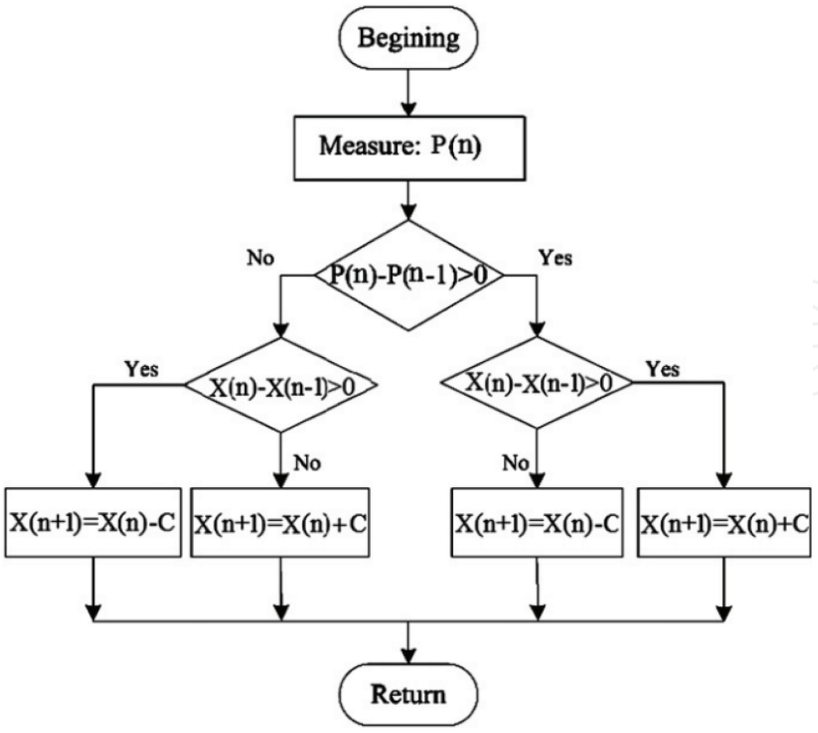

Figure 7. Perturbation and observation algorithm [4].

A small sinusoidal current represented by $\Delta I = a\sin(wt)$ is supposed and added to the reference current (I_{ref}) as a perturbation. This leads to making a ripple on the power (ΔP), whose phase and amplitude are dependent on the relative location of the operating point relative to the MPP. The sinusoidal current perturbation will be added to the reference current and applied to the PV system, as it is clear in **Figure 8**. If the resulting ripple in the current is in phase with the output power ripple, the output power will fall to the left of MPP, and the reference current will be less than I_{MPP}; therefore, the controller will increase the reference current.

On the other hand, if the ripple in the current is not in the same phase with that in the output power, the output power will drop down to the right of MPP, and the reference current will exceed the I_{MPP}. As a result, the controller will reduce the reference current until reaching MPP. The ripple power (ΔP) can be extracted by passing the output through a high-pass filter. Then, the ripple power is demodulated through multiplication by a sin ($wt- \varphi$) signal. The resulting signal, zeta, is either positive or negative depending on the position in the power output curve. After that, zeta is applied to an integrator in order to modify the value of I_{ref} to reach MPP. In the case of falling in the MPP operating point, the amplitude of the ripple will be negligible, and the output power ripple frequency will be twice as many as the current ripple.

There are two major advantages for ESC approach. The first is the optimization problem involving power maximization that is explicitly solved by using the dynamic adaptation-based feedback control law for a sinusoidal perturbation. Hence, attainable MPP is guaranteed when the control algorithm is convergent. The disadvantage of the ESC method lies in the complexity associated with its implementation as well as the necessity to evaluate signals of relatively low amplitude.

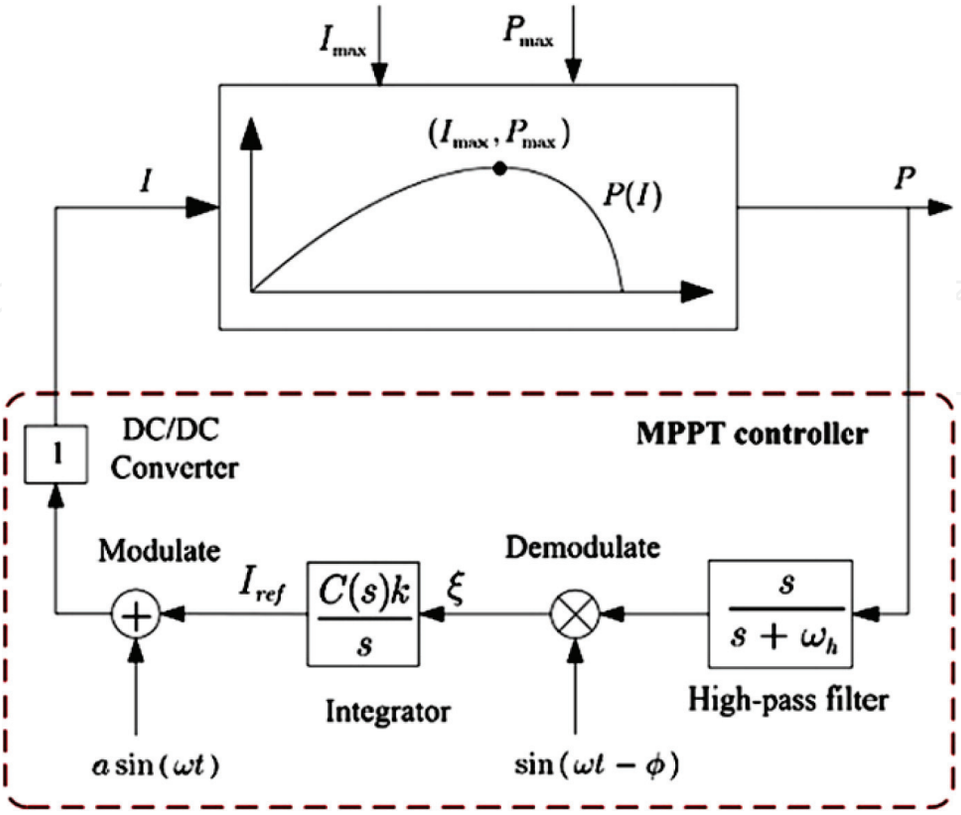

Figure 8. An MPPT controller scheme for the PV system [4].

The method employs the slope of the PV array power characteristics to track MPP that is known as incremental conductance (IncCond) method [12]. In this method, the curve slope of the PV array power is indicated. Based on this, it is zero at the MPP, positive for the output power values, which are smaller than MPP, and negative for values of the output power greater than MPP. The amount of the increment or decrement indicates the MPP tracking speed. An incremental increase may lead to fast tracking, but due to some oscillations around the MPP, the system may not exactly operate at the MPP. That is to say, the usage of IncCond method would be a sort of trade-off between convergence speed and the likelihood of causing oscillations in the MPP.

The main advantage of this algorithm is that it offers an effective solution under rapidly changing atmospheric conditions. The main drawback associated with the IncCond method is that it requires a complex control circuitry.

3.1.3. Hybrid methods

Hybrid MPP methods, a combination of the offline and online methods, are based on tracking of the MPP which are performed in two steps of estimation and exact regulation of MPP. The MPP estimation step relies on offline methods to place the set point close to MPP. The next step, regarded as a fine-tuning step, relying on online methods, attempts to reach the MPP actual value. As expected, the hybrid methods are more efficient to track MPP. In hybrid

methods, the associated control signal has two parts, which are generated based on a separate algorithmic loop.

The first one is determined according to one of the simplified offline methods as a constant value, which depends on the given atmospheric conditions of the PV panel and represents the fixed steady-state value. In this first part, control signal is not intended to track the MPP accurately, while it is required for a fast response to the environmental variations. This part can be generated using one of the previous offline methods or simplifications based on the relationship between output power characteristics and ambient.

The second part obtained based on an online method involving steady-state searches represents attempts to follow MPP exactly. In contrast to the previous part, this second part attempts to reduce the error in steady state and does not require a fast response to the environmental variations. The algorithm, which is provided in **Figure 9**, represents a general description of the hybrid method. As pointed earlier, the first part of the control signal is generated using an offline method through the set-point calculation loop. By employing an online method via the fine-tuning loop, the second part is obtained.

A hybrid method, which has two loops, is presented in [13]. In the first estimation loop based on the open-circuit voltage at a constant temperature, MPP is approximated. In the second precise loop, the P&O method is applied to seek the exact amount of the maximum output power. The transient and steady-state responses are improved by maintaining the small amount of amplitude and frequency of perturbation. The authors in [6] proposed a hybrid approach in which an offline method is used to bring the operating point of the PV array near to the MPP. After that, an online IncCond method is used to track the MPP with high accuracy. Through proper control of the power converter, the initial operating point is set to match a

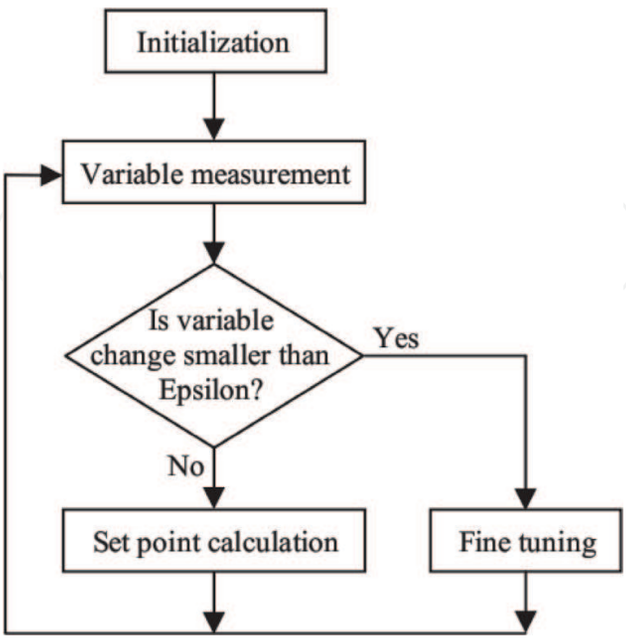

Figure 9. General algorithm of hybrid methods [6].

load resistance proportional to the V_{OC}/I_{SC} ratio associated with the PV array. In this hybrid method, the real MPP tracking is able to ensure that multiple local maxima are presented.

Implementing variable size perturbations by fuzzy logic is a matter of discussion in [14], in the context of achieving improved transient and steady-state responses. The converter duty cycle is adjusted to move the operating point toward the MPP region as soon as possible, thereby improving the response of transient state. A modified P&O algorithm that works based on fuzzy logic and optimized for small variations around the MPP is used simultaneously when MPP region is reached. This method decreases oscillations and increases power produced under the steady-state conditions. Every loop in these chapters applies the P&O approach using perturbations of different amplitude. Here, fuzzy logic decides which loop should be implemented. The peak current control as well as the abovementioned method can result in improving the transient response and decreasing the power loss under steady-state conditions, simultaneously [14].

3.2. DC-link voltage control

One significant feature of the PV-SAF is that typically a DC capacitor is connected between the voltage converter of a PV system and an SAF inverter, rather than a DC source. Because neither PV nor SAF is lossless, a special DC-link voltage controller is required to maintain the DC capacitor average voltage at a constant level. In the PV-SAF, the shunt active filter is usually responsible for this voltage regulation. In the steady state, the average DC-link voltage is maintained at a certain preset level, but during the transient, this is not the case. Such a transient can occur when a change occurred in the output power of a PV plant or a load is either connected or disconnected to/from the SAF. Since it takes a finite-time interval to calculate the new reference current, the shunt compensator cannot immediately respond to the load change. In addition to this, some settling time is required to stabilize the controlled parameter around its reference. Consequently, after a PV output power or a load changing instant, there exists some transient period during which the average voltage across the DC capacitor deviates from its reference value.

Figure 10 shows a strategy of DC-link voltage control in an algorithm, which has two main modes. The first mode would be when the PV produces the power that is ($P_{PV} > P_{min}$) delivered to the network through the SAF, while the second mode is when the threshold P_{min} is more than the power generated by the PV. It needs to be noted that in the two modes, V_{DC} must be greater than V_{min} to have a satisfactory operation of the SAF.

The PV-SAF grid power flow algorithm is illustrated in **Figure 11**. The SAF is like a load that varies when its consumed power is changed with the power generated by PV and the V_{DC}. In the first mode, a boost converter is applied to deliver the generated power of the PV to the DC link. As stated in the control strategy, when threshold voltage ($V_{DC\text{-}min}$) is greater than $V_{DC,}$ the PV power is fed to the DC link in order to maintain it in an acceptable range.

In this situation, the power delivered to the grid through SAF (P_{sh}) is zero; in other words, the power of the PV is solely dedicated to charge the capacitor of the DC link. As V_{DC} exceeded the $V_{DC\text{-}min}$, in order to charge the capacitor, a portion of the P_{PV} is used, and in that case, the rest

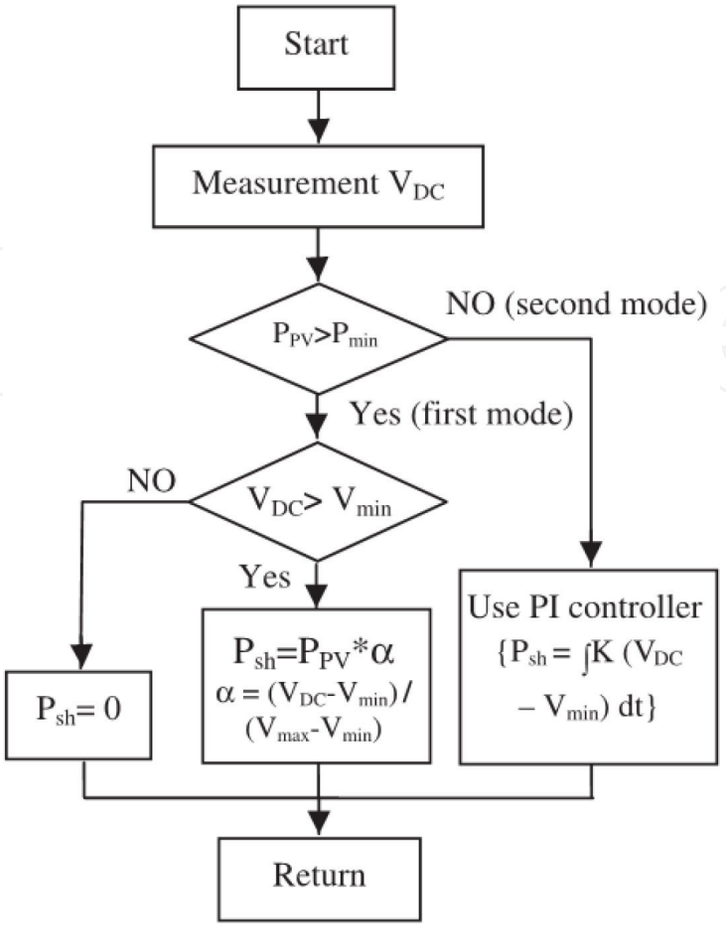

Figure 10. The overall algorithm of the DC-link voltage control [1].

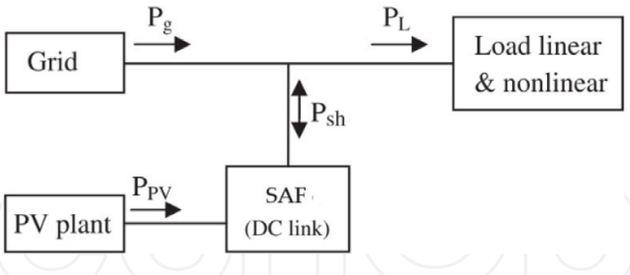

Figure 11. An algorithm of power flow of the PV-SAF [1].

will be delivered to the grid through the parallel part of the SAF. When V_{DC} reaches its maximum and allowable voltage, that is $V_{DC\text{-}max}$, the power of the PV is all fed to the grid.

In the situation that V_{DC} is between $V_{DC\text{-}min}$ and $V_{DC\text{-}max}$ there would be a linear relationship between the power used to charge the capacitor and the $V_{DC\text{-}max}$–V_{DC} ($P_{sh} = \alpha P_{PV}$ and $\alpha = (V_{DC}–V_{min})/(V_{max}–V_{min})$). As a result, some of the load power has been supplied with the PV plant when V_{DC} is greater than $V_{DC\text{-}min}$. Following Kirchhoff's circuit laws, as seen in Eq. (8), the load current (I_{Load}) is equal to the sum of the grid current (Ig) and the SAF current (Ish). Also, SAF current (Ish) is equal to the sum of the PV power plant (I_{PVPP}) and

compensated current (I_C). Here, Eq. (7) can be rewritten to Eq. (9) in order to control the shunt active filter to deliver power of the solar power plant.

$$\begin{aligned} & i_g(t) = i_{Load}(t) - i_{sh}(t) \\ & i_{sh} = i_{pvpp} + i_C \\ & \rightarrow P_g(t) = P_{Load}(t) - P_{sh}(t) \\ & i_{PVPP}(t) = \frac{\overline{P}_{sh}(t)}{U_1{}^+(t).U_1{}^+(t)} U_1{}^+(t) \end{aligned} \tag{8}$$

So, we have

$$\begin{aligned} i_g(t) &= \frac{\overline{P}_g(t)}{U_1{}^+(t).U_1{}^+(t)} U_1{}^+(t) \\ i_C(t) &= i_{Load}(t) - \frac{\overline{P}_g(t) - \overline{P}_{sh}(t)}{U_1{}^+(t).U_1{}^+(t)} U_1{}^+(t) \end{aligned} \tag{9}$$

As addressed in Eq. (9), in addition to providing all negative and zero components of the nonlinear load, SAF will partially provide the positive current component of the nonlinear load, which will result in a lower source current. In the case of a voltage sag, the stored energy in the DC link is fed to the grid through the series part of the SAF. This injected energy enhances the power quality but also causes a decrease in the voltage of the DC link, which will be compensated by the energy given by the PV. In a situation where the PV does not generate power (e.g., $P_{pv} < P_{min}$), the demanded energy to charge the DC link will be provided by the grid.

4. Simulation and discussion

The analysis of the three phases has been done in MATLAB/ SIMULINK environment. The system has a three-phase AC source of 230 V at 50 Hz which is represented as an ideal, balanced, delta, three-phase voltage source, feeding a three-phase nonlinear load (75KVA). The maximum generated power of the PV system is 60 KW.

PV-SAF is utilized for the improvement of power quality in which parallel-connected inverter is operated to perform line current harmonics elimination and reactive power compensation. To study the performance of the proposed algorithm, the results are presented for PV-SAF, where the solar power plant consists of several series-parallel solar panels, which are connected to a boost converter, and delivers the generated power of the solar power plant to the DC link. This power will be delivered by the active filter to a nonlinear load with TDH of more than 40% through a three-phase AC grid with a frequency of 50 Hz and a voltage of 230 V.

Figure 12 shows the voltage and power of solar power plant for MPPT methods of [1, 6]. For both methods of MPPT, an estimation of the operation point is used to set the operation point to a fairly close point near the MPP, and then by means of a fine-tuning loop, MPP will be reached. In the method of [6], the voltage of the MPP is approximated above the actual V_{MPP}

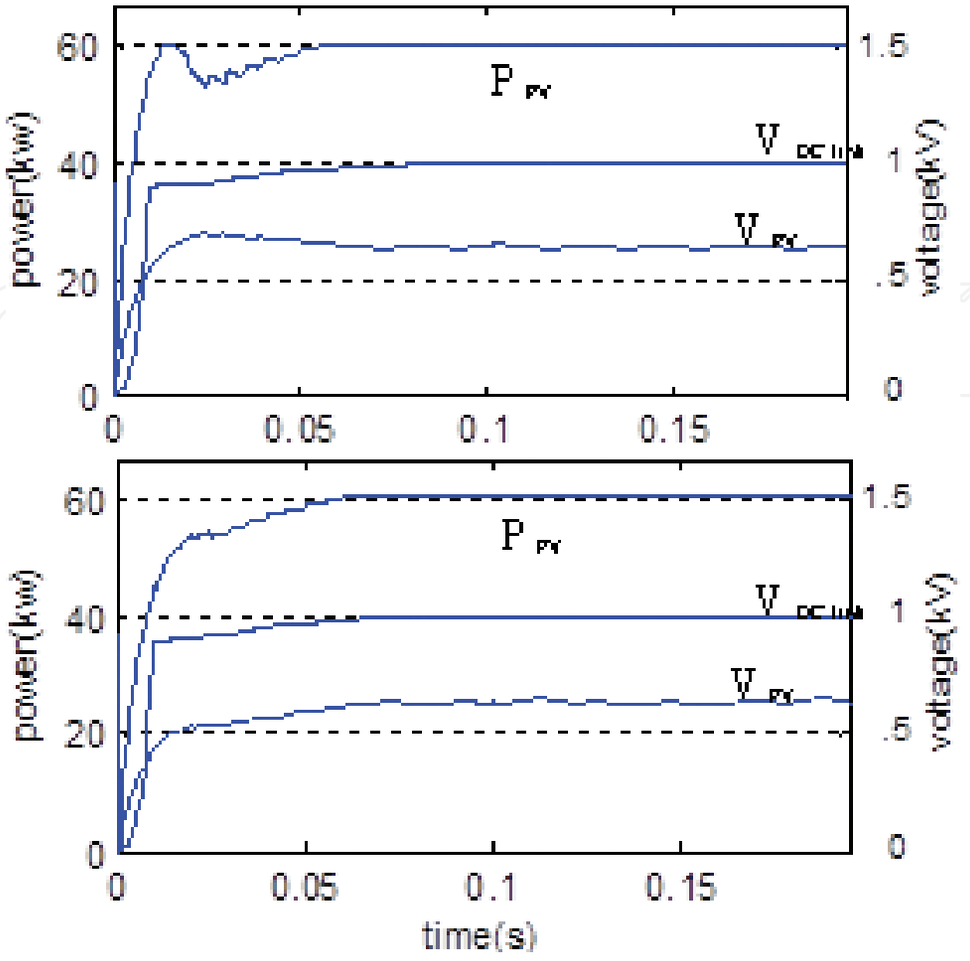

Figure 12. Voltage and power of the PV using MPPT methods of (a) [6] and (b) [1].

operation point consequently, by an increase of V_{DC} from 850 V to 1 KV; the operation point is deviated from MPP and then returns after several milliseconds. It should be noted that the slope of the P-V characteristic curve is greater for voltages more than V_{MPP} in comparison to smaller voltages, meaning that a small change in voltage leads to a great change in the power of the solar panel. It can be seen that in the method of [1], the power smoothly increases until it reaches the MPP. This is because of the independency of the control signal to V_{DC}.

Figure 13, I_{Load}, illustrates the simulated grid current without PV-SAF operation. It is obvious that the grid current is non-sinusoidal and consists of the 50-Hz fundamental component along with lower-order harmonics like the third harmonic (150 Hz), fifth harmonic (250 Hz), seventh harmonic (350 Hz), and so on. **Figure 13**, I_g, shows the grid current with PV-SAF operation. It is clear that the harmonic currents of nonlinear load are almost compensated with the PV-SAF operation so that the line current is nearly a sinusoidal wave. The total harmonic distortion of line current is lower than 4%. **Figure 13**, I_{sh}, shows the injected current of the shunt part of the PV-SAF to compensate the current harmonics of the load so that the grid current can be sinusoidal. Meanwhile, it delivers the power of the PV to the load.

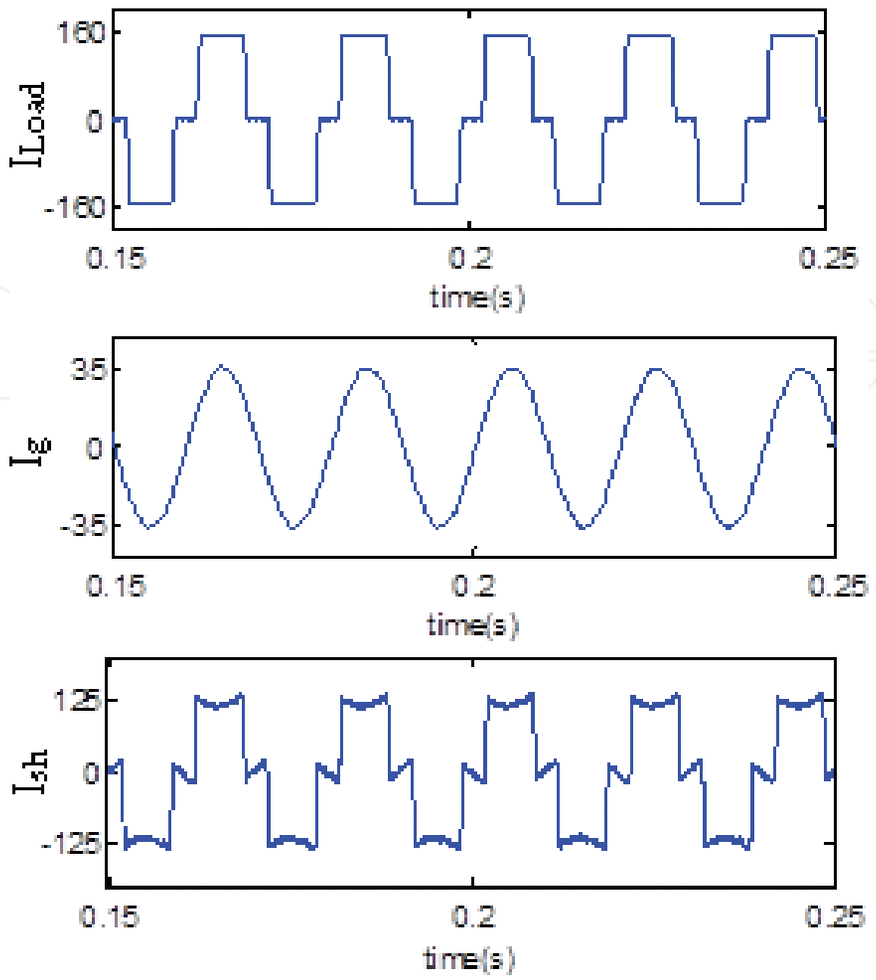

Figure 13. Grid current without PV-SAF (I_{Load}), grid current with PV-SAF (I_g), and the current of part shunt PV-SAF (I_{sh}).

5. Conclusions

In this chapter combined with power conditioner and renewable energy, SAF-PV system has been explained for the optimal designing of PV grid connected. Meanwhile, considering the Advanced Generalized Theory of Instantaneous Power (A-GTIP) algorithm, the SAF-PV system leads to suppress grid-end current harmonics caused by the distorted unbalanced load-terminal voltages. Hence, the grid-end currents could remain purely sinusoidal. Also, PV power is injected to the grid via active filter converter and MV/HV transformer. It means that by using the SAF-PV system, there will be capital investment savings since one less converter and MV/HV transformer will be used in comparison with separated SAF and PV systems. In this chapter, different maximum power point tracking (MPPT) algorithms have also been reviewed which can serve as a guide for the selection of the appropriate MPPT method for specific PV system applications. Various simulation results verify the performance of the combined PV-SAF.

Author details

Ali Reaz Reisi[1]* and Ashkan Alidousti[2]

*Address all correspondence to: reisi.alireza@gmail.com

1 Electrical Engineering Department, Technical and Vocational University, Isfahan, Iran

2 Young Researchers and Elite Club, Shahrekord Branch, Islamic Azad University, Shahrekord, Iran

References

[1] Reisi AR, Moradi MH, Showkati H. Combined photovoltaic and unified power quality controller to improve power quality. Solar Energy. 2013;**88**:154-162

[2] Albuquerque FL, Moraes AJ, Guimara CG, et al. Photovoltaic solar system connected to the electric power grid operating as active power generator and reactive power compensator. Solar Energy. 2010;**84**:1310-1317

[3] Pashajavid E, Bina MT. Zero-sequence component and harmonic compensation in four-wire systems under non-ideal waveforms. Przegląd Elektrotechniczny. 2009;**85**:58-64

[4] Reisi AR, Moradi MH, Jamasb S. Classification and comparison of maximum power point tracking techniques for photovoltaic system: A review. Renewable and Sustainable Energy Reviews. 2013;**19**:433-443

[5] Esram T, Chapman PL. Comparison of photovoltaic array maximum power point tracking techniques. In: IEEE Transactions on Energy Conversion. 2007;**22**(2):439-449. DOI: 10.1109/TEC.2006.874230

[6] Moradi MH, Reisi AR. A hybrid maximum power point tracking method for photovoltaic systems. Solar Energy. 2011;**85**:2965-2976

[7] Zhang C, Zhao D, Wang J, et al. A novel two-mode MPPT method for photovoltaic power generation system. In: IEEE 6th International Conference on Power Electronics and Motion Control. 2009. Wuhan, China: IEEE; 2009. p. 2100-2102

[8] Yang C, Hsieh C, Feng F, Chen K. Highly efficient analog maximum power point tracking (AMPPT) in a photovoltaic system. In: IEEE Transactions on Circuits and Systems I: Regular Papers. July 2012;**59**(7):1546-1556. DOI: 10.1109/TCSI.2011.2177008

[9] Salah CB, Ouali M. Comparison of fuzzy logic and neural network in maximum power point tracker for PV systems. Electric Power Systems Research. 2011;**81**:43-50

[10] Abdelsalam AK, Massoud AM, Ahmed S, Enjeti PN. High-performance adaptive perturb and observe MPPT technique for photovoltaic-based micro grids. In: IEEE Transactions on Power Electronics. 2011;**26**(4):1010-1021. DOI: 10.1109/TPEL.2011.2106221

[11] Lei P, Li Y, Seem JE. Sequential ESC-based global MPPT control for photovoltaic array with variable shading. IEEE Transactions on Power Electronics. 2011;**2**(3):348-358

[12] Mei Q, Shan M, Liu L, Guerrero JM. A novel improved variable step-size incremental-resistance MPPT method for PV systems. In: IEEE Transactions on Industrial Electronics. 2011;**58**(6):2427-2434. DOI: 10.1109/TIE.2010.2064275

[13] NSD' Souza LAC, Liu LXJ. Comparative study of variable size perturbation and observation maximum power point trackers for PV systems. Electric Power Systems Research. 2010;**80**:296-305

[14] Kobayashi K, Takano I, Sawada Y. A study on a two stage maximum power point tracking control of a photovoltaic system under partially shaded insolation conditions. In: IEEE Power Engineering Society General Meeting. Vol. 4; 2003. pp. 2612-2617

IntechOpen